

Observational Studies of Early-type Overcontact Binaries: TU Muscae

Dirk Terrell

*Department of Space Studies, Southwest Research Institute,
1050 Walnut St., Suite 400, Boulder, CO 80302*
terrell@boulder.swri.edu

Ulisse Munari

Osservatorio Astronomico di Padova, Sede di Asiago, I-36032 Asiago (VI), Italy
munari@pd.astro.it

Tomaž Zwitter

Department of Physics, University of Ljubljana, Jadranska 19, 1000 Ljubljana, Slovenia
tomaz.zwitter@fmf.uni-lj.si

Robert H. Nelson

1393 Garvin Street, Prince George, BC, Canada, V2M 3Z1
bob.nelson@shaw.ca

ABSTRACT

We present new spectroscopic and photometric data on the early-type overcontact binary TU Muscae. The analysis of the spectroscopic data shows that the line of sight to the system crosses three kinematically sharp and well-separated interstellar reddening sources and that the stars rotate synchronously. We present new radial velocities that are in good agreement with earlier optical velocities and, thus, do not confirm the systematically smaller velocities obtained from IUE spectra. The optical velocities are analyzed simultaneously with the photometric data to derive accurate absolute dimensions for the binary components. The results show that TU Mus consists of an O7.5 primary with $M_1 = 23.5 \pm 0.8 M_\odot$, $R_1 = 7.48 \pm 0.08 R_\odot$ and an O9.5 secondary with $M_2 = 15.3 \pm 0.4 M_\odot$, $R_2 = 6.15 \pm 0.07 R_\odot$ in an overcontact configuration and that the orbital period has remained constant over the three decades covered by the observations. These results might imply that the mass transfer seen in late-type overcontact binaries does not occur in their early-type counterparts.

Subject headings: binaries: eclipsing — binaries: spectroscopic — stars: individual (TU Mus) — stars: main sequence

1. Introduction

The variability of TU Muscae (HD 100213) was discovered by Oosterhoff (1928) and the system was first studied in detail by Andersen &

Grønbech (1975, hereafter AG75) who list references to earlier work on this early-type overcontact (Wilson 2001) binary. Given the paucity of eclipsing, double-lined O-type binaries, TU Mus has received surprisingly little attention from observers.

AG75 published fully covered *uvby* light curves and fourteen radial velocities for each star near quadratures from photographic spectra of moderate resolution. Stickland, et al. (1995, hereafter S95) presented twenty-four radial velocities for the primary star and twenty-three for the secondary from high resolution International Ultraviolet Explorer (IUE) spectra. TU Mus was bright enough ($V_T = 8.4$) to be observed by Hipparcos and a light curve with about a hundred points was published in the Hipparcos Epoch Photometry Annex (ESA 1997). Two analyses of these data using modern light curve synthesis tools have been published: a preliminary report on the current work by Terrell (2002) and an analysis of the AG75 photometry by Wilson & Rafert (1981).

The two sets of radial velocities give quite discrepant results for the absolute dimensions. AG75 obtained photographic spectra with a dispersion of 20 \AA mm^{-1} and found $K_1=251.3 \pm 4.8 \text{ km sec}^{-1}$ and $K_2=370.5 \pm 4.3 \text{ km sec}^{-1}$. S95 found $K_1=216.7 \pm 2.7 \text{ km sec}^{-1}$ and $K_2=345.4 \pm 3.1 \text{ km sec}^{-1}$ from their IUE spectra that had signal-to-noise ratios (S/N) of 10-20. Adopting an inclination of 76° , these numbers result in masses of $M_1 = 17.2M_\odot$ and $M_2 = 10.8M_\odot$ for the IUE velocities and $M_1 = 23.5M_\odot$ and $M_2 = 15.8M_\odot$ for the optical velocities, a difference much larger than the error limits allow. In order to explore the nature of this discrepancy, we obtained high-resolution, high S/N spectra of TU Mus near the quadratures. Although we have a limited number of spectra due to the difficulty of obtaining observing time on large telescopes for the study of eclipsing binaries, we find very good agreement with the AG75 results.

Given the good agreement between our velocities and those of AG75, we performed a simultaneous solution of those velocities, the AG75 *uvby* photometry, the Hipparcos photometry and new *BV* photometry from the 2002 observing season. We used the 2003 version of the Wilson-Devinney (WD) program (Wilson & Devinney (1971), Wilson (1979), Wilson (1990)) and present new elements for the binary, showing that the period has remained remarkably constant over the roughly thirty year span of all the observations.

2. Spectroscopy

Nine ESO 2.2m + FEROS spectra have been secured, in three groups of three spectra each (Table 1). The wavelength range of the spectra extends from 3900 \AA to 9200 \AA with $R = 48,000$ and a 400 second exposure time. The S/N is evaluated around $H\beta$ and the orbital phase is computed with the ephemeris given in section 4.

2.1. Rotational velocity

AG75 estimated the rotational velocities of the primary and secondary stars in TU Mus as 285 and 240 km sec^{-1} ($\pm 10\%$), while S95 derived significantly slower rotations: 250 and 195 km sec^{-1} ($\pm 10\%$), respectively. To derive the rotational velocity we used the relation

$$V_{\text{rot}} = 42.42 \times HIW - 35 \text{ km sec}^{-1} \quad (1)$$

calibrated by Munari & Tomasella (1999) on the width at half maximum of He I 5876 \AA in high resolution spectra of O and B stars. The deconvolution of the He I 5876 \AA line profile in the two TU Mus quadrature spectra gives a HIW of 7.26 and 7.35 \AA for the primary, and 6.37 and 6.36 \AA for the secondary, which corresponds to 273 and 277 , and 234 and 236 km sec^{-1} respectively. The Munari and Tomasella relation was calibrated using single, and thus axially symmetric, stars. The components of TU Mus depart quite strongly from axial symmetry so we investigated its influence on the HIW using the line profile feature of WD. We computed the HIW for TU Mus and for a spherical star with radius equal to the r_{back} radii of the TU Mus components. We found that the HIW for TU Mus was about 5% smaller than for the spherical star. Applying this correction to our data, we adopt 290 and 248 km sec^{-1} as the rotational velocities of primary and secondary. Of course, the concept of a rotational velocity is of less obvious usefulness for stars like TU Mus than for axially symmetric ones. The question arises as to where on the equator of TU Mus the above rotational velocities apply. Since our spectra were taken at quadrature phases, r_{back} seems appropriate and we find values of 291 and 242 km sec^{-1} there from our light curve solution (which assumed synchronism), in excellent agreement with the line profile results. Our data support the AG75 values and rule out the smaller values measured by S95.

TABLE 1
ESO 2.2M + FEROS SPECTRA OF TU MUS

Spectrum Number	Date	UT of mid-exposure	S/N	Orbital Phase
1346, 1347, 1348	Feb 22, 2003	07:08:56, 07:18:16, 07:27:31	75, 68, 72	0.032
1629, 1630, 1631	Feb 25, 2003	06:07:24, 06:16:39, 06:25:59	160, 165, 158	0.211
1693, 1694, 1695	Feb 26, 2003	00:45:27, 00:54:47, 01:04:07	125, 130, 120	0.771

To confirm the MT method we have applied it to the He I 5876 Å line of the B1.5Vn star HIP 77635 that we observed under identical instrumental conditions soon after TU Mus on Feb. 22. Its rotational velocity is reported as 306 km sec⁻¹ in the Bernacca & Perinotto (1970) catalogue of rotational velocities. The HIW of the line turned out to be 8.16 Å which corresponds to 311 km sec⁻¹ according to Equation 1. This excellent agreement supports our confidence in the rotational velocities we have measured for the components of TU Mus. We have also computed synthetic, broadened profiles for He I 4471, 6678 and 7065 Å and the agreement with the observed profiles is also excellent.

2.2. Distance

Assuming a luminosity ratio $L_2/L_1=0.55$ from our light curve solution, the $V_T=8.41$ magnitude transforms into Johnson V magnitudes of $V_1=8.88$ and $V_2=9.52$, following Bessell (2000). With $E_{B-V}=0.19$ (see below) and assuming an O7.5V classification for the primary, the distance to TU Mus amounts to 4.77 kpc using the absolute magnitudes calibrated by Houk, Branch & Winfrey (1994) ($M_V=-5.1$, -4.5 for O7.5V, O9.5V stars) and a ratio of total to selective absorption of $R_V = 3.1$. The same calculation for the O9.5V secondary results in a distance of 4.86 kpc. We therefore adopt 4.8 kpc as the distance to TU Mus.

2.3. Reddening

The interstellar lines of Na I offer a means of estimating the reddening affecting TU Mus independent of the knowledge of the intrinsic colors. The profile of Na I D1 and D2 lines on our FEROS spectra of TU Mus are shown in Figure 1. They are clearly composed of three separate components. Their average position, width and equivalent

width have been derived from multi-Gaussian fitting on all 9 available spectra, and the results are summarized in Table 2, where the errors are the standard errors. The 9 individual spectra gave extremely consistent results. The multi-Gaussian *mean* fit of Table 2 is overplotted on the D2 line of spectrum #1629 in Figure 1 to show the accuracy of the fit.

The equivalent widths of the three components have been transformed in Table 2 into the corresponding color excess using the relation calibrated by Munari & Zwitter (1997), with a total color excess amounting to $E_{B-V}=0.19\pm 0.01$. Similar profiles are observed for K I 7698 Å and H & K Ca II interstellar lines. The Na I widths in Table 2 are not corrected for instrumental width, which amount to 5.0 km sec⁻¹ from unresolved telluric lines in the vicinity of Na I lines (thus intrinsic width does not exceed 3 km sec⁻¹). The line of sight to TU Mus therefore crosses three kinematically very sharp and well separated sources of reddening, of pure interstellar origin. In fact none of the components show radial velocity change with orbital phase and none share the -4 km sec⁻¹ systemic velocity.

Of interest is the heliocentric radial velocity of the three components. The accuracy reported in Table 2 is not fictitious because nearby telluric absorptions show the same wavelength stability from one spectrum to the other, and it matches the expected high FEROS spectrograph stability suitable for extra-solar planet searches. The limited resolution of the AG75 spectra did not allow them to recognize the multi-component structure of the interstellar lines (H and K lines of Ca II), for which they estimated a -7.3 ± 0.8 km sec⁻¹ radial velocity. Averaging the three components in Table 2 weighted according to equivalent width, a radial velocity of -0.7 ± 0.2 km sec⁻¹ is derived for an unresolved interstellar Na I profile. However,

TABLE 2
COMPONENTS OF THE INTERSTELLAR LINES IN THE TU MUS SPECTRUM

Quantity	Component 1	Component 2	Component 3	Total
RV (km sec ⁻¹)	-15.51±0.09	+5.8±0.2	+15.6±0.1	
Width (km sec ⁻¹) ^a	6.00±0.04	5.8±0.1	5.3±0.2	
Na I D2 E.W. (Å)	0.225±0.002	0.216±0.002	0.099±0.003	
$E_{(B-V)_i}$	0.080	0.075	0.031	0.19±0.01

^aUncorrected for the dominating ~ 5.0 km sec⁻¹ instrumental width

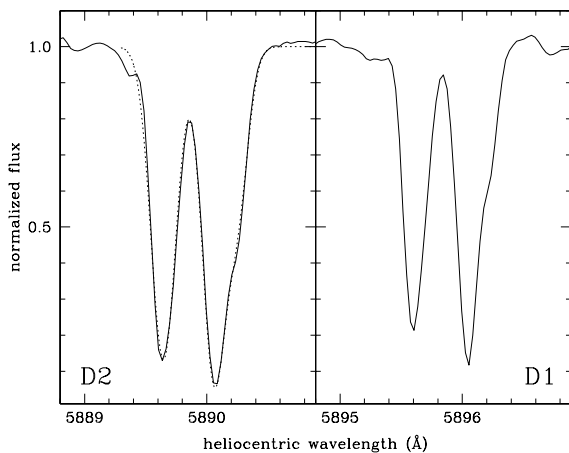


Fig. 1.— The interstellar lines of Na I D (spectrum #1629) with superimposed the three-component Gaussian fitting of Table 2.

a -7.2 ± 0.4 km sec⁻¹ value averaged by equivalent width is obtained on our spectra for both H & K Ca II as well as K I interstellar lines. While showing exactly the same two major components of Na I D1 & D2, they fail to show the third, reddest one.

The radial velocities of the three components are plotted in Figure 2 where they are compared with the expected values of the mean galactic rotation along the line of sight to TU Mus ($l=284.8$, $b=-4.1$ deg) from the Hron (1987) formalism with $A=-17$ km sec⁻¹ and $\alpha=-2.0$ km sec⁻¹ pc⁻² and Pont, et al. (1994) values for (u_o, v_o, w_o) . It is evident that the mean Galaxy rotation curve does not reproduce the expected velocities up to the ~ 4.8 kpc distance to TU Mus (note that the line of sight to the target is still mostly within the $z = \pm 150$ pc dust layer around the galactic plane

at the estimated ~ 4.8 kpc distance). The discrete velocity field maps of Brand & Blitz (1993), based on H II regions and reflection nebulae, do not perform much better, which could be anticipated given the scant and widely spaced data used in their analysis in that part of the Galaxy. Only the stronger component can be accounted for and located at ~ 2.5 kpc distance by the Brand & Blitz (1993) map. The limited individual reddening implied by the equivalent widths of the three interstellar lines suggests that only a few limited and kinematically scattered bubbles of the interstellar medium are crossed by the line of sight, with a diffuse component playing a marginal role, if any. The kinematic information from the interstellar

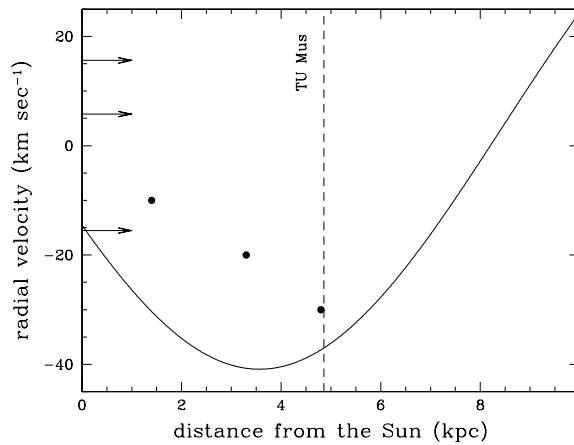


Fig. 2.— The radial velocity of the three components of Na I interstellar lines (arrows) compared with behaviour of the general galactic rotation curve of Hron (1987, continuous line) and the local mapping by Brand and Blitz (1993, solid points) up to the distance of TU Mus (vertical dashed line).

lines cannot therefore be used to constrain the distance to TU Mus.

2.4. Radial velocities

The radial velocity of TU Mus has been measured on the two groups of spectra in Table 1 obtained close to quadrature phases. Those around orbital phase 0.03 are very close to conjunction and thus have insufficient velocity separation between the two components to obtain reliable radial velocities. Line splitting at quadrature is wide and allows an easy and firm determination of the radial velocity, as shown for $H\beta$ in Figure 3. The radial velocities have been obtained by Gaussian de-convolution of the profiles into two components, which provide an excellent overall fit to the observed line profile. The measured lines are He I 4016.218, 4471.507, 4921.929, 5015.675, 5875.651, 6678.149, 7065.276 Å; He II 4199.831, 4541.589, 4685.682, 5411.524 Å; and $H\gamma$, $H\beta$, $H\alpha$. The mean of the radial velocities (and associated standard error) derived from these 14 lines is in Table 3.

Our high dispersion, high S/N radial velocities are very close to the photographic ones by AG75 and definitively rule out the smaller ones obtained by S95 on low S/N IUE SWP high resolution spectra. This is clearly demonstrated by Figure 4 that shows the He I 5876 Å line of spectrum # 1629 superimposed with the two component fit using our radial velocities in Table 3 and the corresponding values for AG75 and S95.

2.5. Spectral classification and metallicity

Both stars are O-type, showing the whole series of expected He II lines. Their spectral types are somewhat different, as the comparison of $H\beta$ and He I 4471 Å profiles in Figures 3 and 4 suggests. The ratio of the two $H\beta$ lines is 1.8 while those of the He I is 1.3, favoring a two spectral subtype higher temperature for the primary. A reasonable estimate seems to be O7.5 for the primary and O9.5 for the secondary.

Other than the hydrogen and helium lines, only two C III lines are clearly visible at 4650 Å and 4069 Å (Si IV lines are unsuitable in this regard.) Both C III lines are actually blends of three individual lines with complicated profiles caused by wide wavelength separation within the triplets,

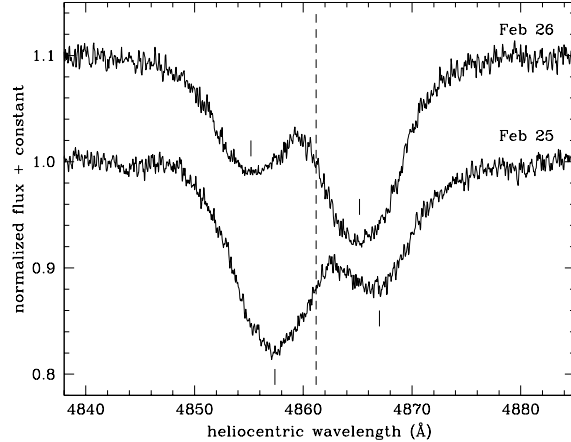


Fig. 3.— The $H\beta$ profile of TU Mus for the averaged Feb 25 and Feb 26 spectra of Table 1. The ticks mark the primary and secondary radial velocity from Table 3.

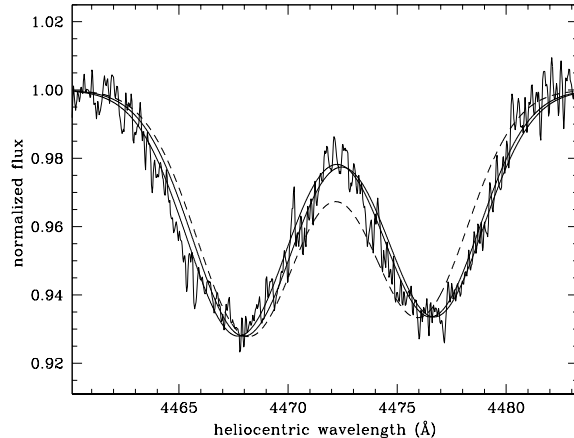


Fig. 4.— The He I 4471 Å profile for Feb 25 spectra of Table 1, superposed with the double Gaussian fitting with our velocities from Table 3 (thick solid line), corresponding AG75 velocities (thin solid line) and S95 ones (dashed line).

TABLE 3
HELIOCENTRIC RADIAL VELOCITIES OF TU MUS

Spectrum Number	Orbital Phase	Primary			Secondary		
		This Paper	AG75	S95	This Paper	AG75	S95
1629-30-31	0.211	-244 ± 5	-246	-225	$+350 \pm 5$	+364	+324
1693-94-95	0.771	$+237 \pm 4$	+249	+197	-380 ± 8	-362	-348

fast rotation, and the SB2 nature of the spectra. However, a comparison with synthetic spectra does not support a carbon content, and therefore metallicity, far from the solar value.

3. Photometry

TU Mus was observed by RHN on 10 nights from 2002 April 13 to June 4 at the Mount John University Observatory while he was a guest of the University of Canterbury in Christchurch, New Zealand. The f/13.5 Cassegrain focus on the 0.61 meter Optical Craftsmen telescope was used together with a Santa Barbara Instrument Group ST-9E CCD camera, utilizing the KAF-0261E chip (512x512) with 20 micron pixels. A tele-compressor lens operated at 2.11x compression reduced the focal ratio to 6.4 and gave a field of view of $9' \times 9'$. The B and V (Johnson) filters were by Schuler.

Reduction of the CCD images and aperture photometry was done with the MIRA software package.¹ Bias and dark removal plus flat fielding (dome flats) were done in the usual way. The comparison star was GSC 8984:0579 and the check stars were GSC 8984:1473 and GSC 8984:1623. Weather and time constraints did not permit the determination of transformations to the standard system. There were 1973 frames taken in B and 1962 in V. However, wispy clouds often caused scattered measurements. In order to remove errant measurements in an objective way, the raw comparison magnitudes were plotted versus time. Points adjacent to rapidly changing values (greater than 0.2 magnitudes per sampling interval of 30 seconds) were rejected. In this way,

the data set was reduced to 1148 points in B and 1493 points in V, and the light curves were cleaned up considerably.

4. Data Analysis

We performed a simultaneous analysis of the AG75 photometry and radial velocities, the Hipparcos photometry, and our new photometry and velocities with the 2003 version of the Wilson-Devinney (WD) code. This version of WD has the capability of modeling the radiation of the stars by Kurucz (1993) atmospheres and we used this feature in our solutions.

In early exploratory fits with the light curve program of WD, it became clear that the AG75 photometry, the Hipparcos photometry, and our new photometry were not consistent in terms of the depths of the eclipses. The AG75 and Hipparcos photometry matched well, but our new photometry had slightly deeper eclipses, requiring an inclination about one degree higher. Rather than indicating some real change in the inclination of the system, the differences result from the fact that the older photometry suffers from third light contamination. The Digitized Sky Survey image of the field shows a companion about $15''$ southeast of TU Mus. Our aperture photometry was done with a $10''$ aperture and therefore did not include the companion. The effective aperture for the Hipparcos observations was about $30''$ (ESA 1997), thus including the companion. The AG75 data also included the companion since their aperture was $30''$. The Guide Star Catalog lists the brightness of the companion as $13^m 0 \pm 0^m 4$. In our light curve solutions below, we allowed for third light in all of the photometry but the values for the *BV* curves were always very tiny, thus we conclude

¹Available at <http://www.axres.com>

that third light does not affect our BV data. The solution did find third light in the AG75 and Hipparcos data and the results are consistent with the GSC brightness of the companion. Figure 5 shows the DSS image of the area around TU Mus.

Previously, WD had been modified to allow for the use of either binary phase or time as the independent variable (Wilson & Terrell 1998). In the latter case, one can solve for the orbital period (P), its first time derivative (\dot{P}), and the reference epoch (HJD_0 , usually the time of primary minimum). In order to investigate the behavior of the period of TU Mus, we used time as the independent variable for our simultaneous solutions, adjusting the period and reference epoch. Attempts to adjust \dot{P} always resulted in values statistically indistinguishable from zero, indicating that the period of TU Mus has remained constant over the thirty year span of the observations being analyzed. Our estimate of the ephemeris is

$$HJD_{min} = 2448500.3080(1) + 1.38728653(2) \times E \quad (2)$$

for primary eclipse where the quantities in parentheses are the 1σ uncertainties in the last digits of the parameters.

Other parameters adjusted in the simultaneous solution were the semi-major axis of the relative orbit (a), the binary center of mass radial velocity (V_γ), orbital inclination (i), secondary mean effective temperature (T_2), common envelope surface potential (Ω), mass ratio (q), and the bandpass-specific luminosity of the primary (L_1). Other parameters, such as the bolometric albedos and gravity brightening exponents, were held fixed at their expected theoretical values. The square root limb darkening law was used with coefficients from Van Hamme (1993). The mean effective temperature of the primary was set to 35,000 K based on the O7.5 spectral type. Data set weights were determined by the scatter of the observations. WD gives output at each step from which the standard deviations of the data sets, σ , can be calculated. It is sufficient to determine reasonably good starting values for the standard deviations by examining plots of the observations and then adjust them as the solution progresses. Within a given light curve or radial velocity curve, WD can also apply individual weights. For the radial velocities, we set the base curve weights for the AG75 velocities

and then gave our new velocities higher individual weights based on their estimated errors. In order to eliminate potential local minimum problems, we began the solutions from several starting points and found that the same minimum was always recovered.

Table 4 shows the results of the simultaneous solution. TU Mus is just barely in an overcontact configuration, having a surface potential of 3.137 ± 0.002 while the inner critical potential is 3.156 for the estimated mass ratio of 0.651. Using the degree of contact index defined by Wilson & Rafert (1981), where point contact has a value of 1.0, we find a value of 1.006 for TU Mus. Figure 6 shows the fit to the AG75 radial velocities and the ones we obtained. The fit to the Hipparcos photometry is shown in Figure 7 and since all of the various observations were phased with the ephemeris given in Equation 2, it shows that the period has remained constant to the precision with which we can measure it. Figure 8 shows the fit to the AG75 u observations and exhibits a small but noticeable asymmetry in the maxima, a phenomenon frequently seen in the light curves of late-type overcontact (W UMa) systems. As can be seen in Figure 9, the asymmetry is slightly smaller in the y data, indicating that the source of the asymmetry is a high temperature phenomenon, perhaps a superluminous area as suggested in CE Leo by Samec, et al. (1993) and YZ Phe by Samec & Terrell (1995). Figure 10 shows the fits to our B and V data. An asymmetry is present in these newer data but in the opposite sense from the AG75 data, indicating that the source of the asymmetry is variable in time.

5. Age and Evolutionary Status

Very little is known about the structure and evolution of overcontact binaries with radiative envelopes. To our knowledge, no models of this type have been published. Although obviously limited, a comparison with single-star models can be instructive in estimating the age and evolutionary status of TU Mus. Using a stellar evolution code (Han, et al. (1994), Eggleton (1973), Eggleton (1972), Eggleton (1971)) kindly supplied to us by P. Eggleton, we have constructed evolutionary models of $23.5M_\odot$ and $15.3M_\odot$. The model for the primary reaches the observed radius of the TU

TABLE 4
PARAMETERS OF TU MUS

Parameter	Value ^a
a	$17.7 \pm 0.2 R_{\odot}$
V_{γ}	$-4 \pm 4 \text{ km sec}^{-1}$
i	$77^{\circ}8 \pm 0^{\circ}1$
T_1	35,000 K
T_2	$31,366 \pm 16 \text{ K}$
Ω_1	3.137 ± 0.002
q	0.651 ± 0.001
HJD_0	2448500.3066 ± 0.0001
P	$1.38728653 \pm 0.00000002 \text{ days}$
$L_1/(L_1 + L_2)_{HP}$	0.648 ± 0.006
$L_1/(L_1 + L_2)_u$	0.659 ± 0.003
$L_1/(L_1 + L_2)_v$	0.648 ± 0.003
$L_1/(L_1 + L_2)_b$	0.646 ± 0.003
$L_1/(L_1 + L_2)_y$	0.646 ± 0.003
$L_1/(L_1 + L_2)_B$	0.648 ± 0.003
$L_1/(L_1 + L_2)_V$	0.646 ± 0.003
$l_3(HP)$	0.030 ± 0.007^b
$l_3(u)$	0.023 ± 0.004
$l_3(v)$	0.023 ± 0.004
$l_3(b)$	0.025 ± 0.004
$l_3(y)$	0.026 ± 0.004
R_1	$7.48 \pm 0.08 R_{\odot}$
R_2	$6.15 \pm 0.07 R_{\odot}$
M_1	$23.5 \pm 0.8 M_{\odot}$
M_2	$15.3 \pm 0.4 M_{\odot}$
$\log L_1/L_{\odot}$	4.8 ± 0.2^c
$\log L_2/L_{\odot}$	4.5 ± 0.2

^aQuoted errors are 1- σ errors.

^b l_3 values are in units of total system light at phase 0.25.

^cThe luminosity errors are estimates based on the uncertainty of a few thousand K in the effective temperature of the primary. The error contributions to the luminosities due to the errors in the radii are more than an order of magnitude smaller.

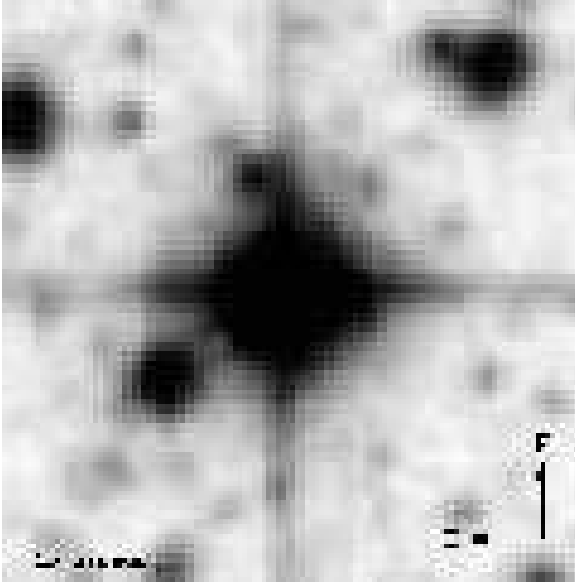


Fig. 5.— The Digitized Sky Survey image of the TU Mus field showing the companion approximately $15''$ to the southeast.

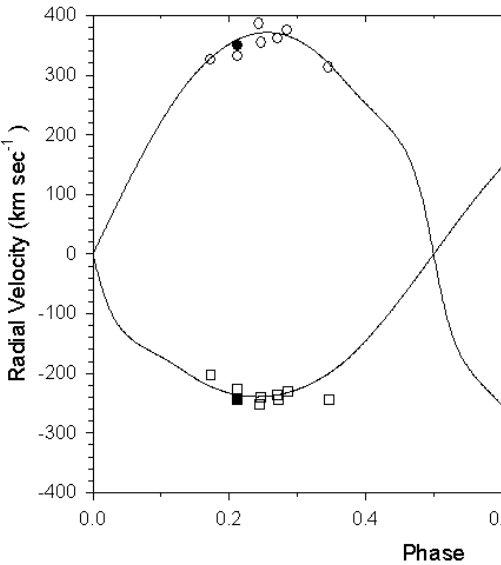


Fig. 6.— The fit to the radial velocities from this paper (solid symbols) and those of AG75 (open symbols).

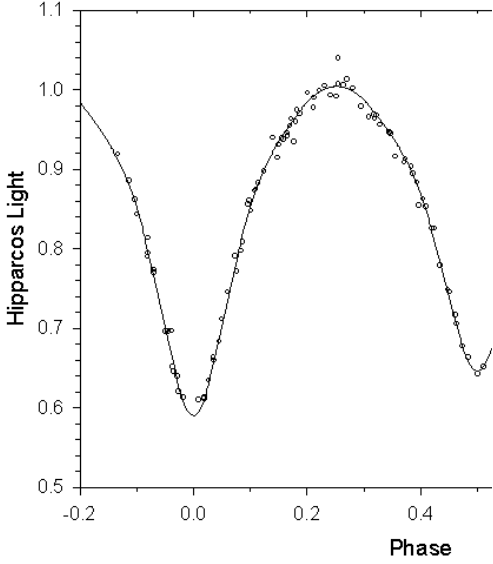


Fig. 7.— The fit to the Hipparcos observations using the parameters of Table 4.

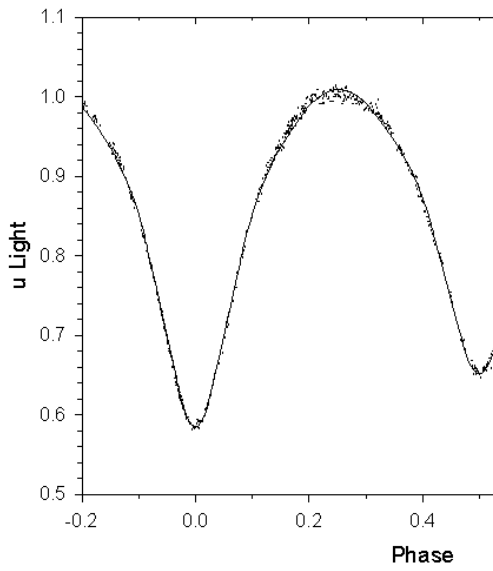


Fig. 8.— The fit to the AG75 u observations using the parameters of Table 4.

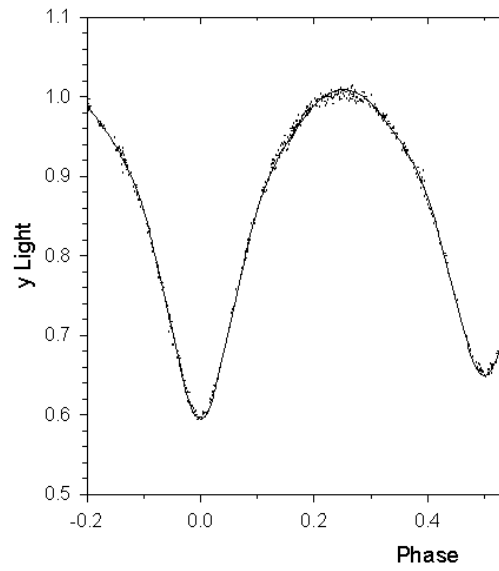


Fig. 9.— The fit to the AG75 y observations using the parameters of Table 4.

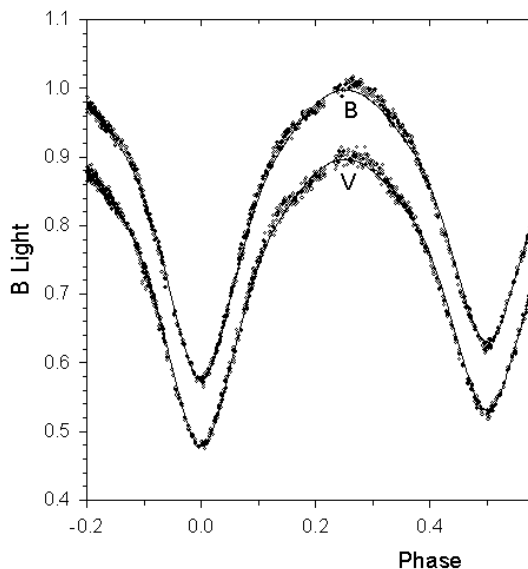


Fig. 10.— The fit to our new BV observations using the parameters of Table 4.

Mus primary at about 2.6 Myr and the model for the secondary reaches the observed radius at about 6.2 Myr. Because of the luminosity exchange from the primary to the secondary, the radius of the primary is probably less than it would be without the luminosity transfer. Similarly, the secondary is probably larger than it otherwise would be. Thus the true age of TU Mus probably lies between these two values. Our ignorance of the structure and evolution of these stars is so great, however, that one cannot discount the possibility that the current configuration is a result of a much more complicated evolutionary history.

Two results from this work, the overcontact configuration and the lack of any period change, have interesting implications for the structure of early-type overcontact systems. In the late-type overcontact (W UMa) systems, the luminosity transfer drives mass transfer from the less massive to the more massive star, resulting in period changes. But if TU Mus truly is in an overcontact configuration, the same level of mass transfer cannot be taking place because of the constant period. What is clearly needed is more work in this area with modern codes like Djehuty (Eggleton, et al. 2003). More sophisticated modeling by 3D stellar evolution codes will certainly give us a better understanding of the structure and evolution of early-type overcontact systems and the well-determined properties of TU Mus makes it a good target of such modeling.

6. Conclusions

Our analysis of new and existing data on TU Mus shows it to be an overcontact binary consisting of a $23.5M_{\odot}$ primary and a $15.3M_{\odot}$ secondary with a small degree of contact. Our results are in very good agreement with the results of AG75 and contradict the smaller masses found by S95. The source of the discrepancy between the UV and optical velocities is not clear. One idea we explored was the effect of the change in the center of light due to the reflection effect between the UV and optical, but our experiments indicated that this effect is much too small to explain the large discrepancy. Given our agreement with the AG75 velocities, one is left with two possible conclusions: that the UV velocities suffer from some unrecognized systematic error or there is some fundamental ef-

fect that causes a difference between UV and optical velocities for stars of this type. We note that Stickland and colleagues have seen a similar discrepancy for LY Aur (Stickland, et al. 1994). Our current understanding of the structure and evolution of early-type overcontact binaries is quite limited and we hope that our results for the observed properties of TU Mus may serve as a good test of future 3D models of these stars.

RHN thanks the American Association of Variable Star Observers for the loan of the ST-9E camera. RHN would also like to thank specifically the two technicians at the observatory, Alan Gilmore and Pam Kilmartin, for their superb help, and the members of the Physics and Astronomy Department at the University of Canterbury for their warm hospitality. This research has made use of the SIMBAD database, operated at CDS, Strasbourg, France.

REFERENCES

- Andersen, J. & Grønbech, B. 1975, *A&A*, 45, 107 (AG75)
- Bernacca, P.L. & Perinotto, M. 1970, *Contr. Oss. Astrof. Padova in Asiago*, 239, 1
- Bessell, M. S. 2000, *PASP*, 112, 961
- Brand, J. & Blitz, L. 1993, *A&A*, 275, 67
- Eggleton, P. P. 1971, *MNRAS*, 151, 351
- Eggleton, P. P. 1972, *MNRAS*, 156, 361
- Eggleton, P. P. 1973, *MNRAS*, 163, 279
- Eggleton, P. P., et al. 2003, in *3D Stellar Evolution*, ed. S. Turcotte, S. C. Keller and R. M. Cavallo (San Francisco: ASP), 15
- ESA 1997, *The Hipparcos and Tycho Catalogues*, ESA SP-1200
- Flower, P. J. 1996, *ApJ*, 469, 355
- Han, Z., Podsiadlowski, P. and Eggleton, P. P. 1994, *MNRAS*, 270, 121
- Houk, N, Branch, C. & Winfrey, S. 1994, *BAAS*, 26, 1449
- Hron, J. 1987, *A&A*, 176, 34
- Kurucz, R. L. 1993, in *Light Curve Modeling of Eclipsing Binary Stars*, ed. E. F. Milone (New York: Springer-Verlag), 93
- Marquardt, D. W. 1963, *J. Soc. Indust. Appl. Math.*, 106, 2096
- Munari, U. & Tomasella, L. 1999, *A&A*, 343, 806
- Munari, U. & Zwitter, T. 1997, *A&A*, 318, 269
- Oosterhoff. P. T. 1928, *Bull. Astron. Inst. Neth.* 4, 183
- Pont, F., Mayor, M., & Burki, G. 1994, *A&A*, 285, 415
- Samec, R. G.; Su, W., Terrell, D., & Hube, D. P. 1993, *AJ*, 106, 318
- Samec, R. G. and Terrell, D. 1995, *PASP*, 107, 427
- Stickland, D. J., Lloyd, C., Koch, R. H., & Pachoulakis, I. 1995, *The Observatory*, 115, 317 (S95)
- Stickland, D. J., Z Koch, R. H., Pachoulakis, I., & Pfeiffer, R. J. 1995, *The Observatory*, 114, 107
- Terrell, D. 2002, in *ASP Conf. Ser. 297, Exotic Stars as Challenges to Evolution*, ed. C. A. Tout & W. Van Hamme (San Francisco: ASP), 319
- Van Hamme, W. 1993, *AJ*, 106, 2096
- Van Hamme, W. & Wilson, R. E. 1984, *A&A*, 141, 1
- Wilson, R. E. 1979, *ApJ*, 234, 1054
- Wilson, R. E. 1990, *ApJ*, 356, 613
- Wilson, R. E. 2001, *Inf. Bull. Variable Stars*, No. 5076
- Wilson, R. E & Biermann P. 1971, *A&A*, 48, 349
- Wilson, R. E & Devinney, E. J. 1971, *ApJ*, 166, 605 (WD)
- Wilson, R. E & Rafert, J. B. 1981, *Ap&SS*, 76, 23
- Wilson, R. E & Terrell, D. 1998, *MNRAS*, 296, 33